École Normale Supérieure Paris-Saclay
Département de Biologie

Rapport final

Année ARPE 2017-2018

Dynamics of fish schooling behaviour in relation to predator abundance

Thelma PANAÏOTIS

2 octobre 2017 – 29 juin 2018

Sous la direction de
Prof. Jessica MEEUWIG, Dr. Phil BOUCHET et Dr. Shanta BARLEY

Centre for Marine Futures
School of Biological Sciences
University of Western Australia (M092)
35 Stirling Highway
Crawley 6009, Australia

Table of contents

List of abbreviations

AIC: Akaike information criterion

BFAS: proportion of fish on border of alpha shape

BFCH: proportion of fish on border of convex hull

BRUVS: baited remote underwater video system

FL: fork length

FN: fish number

GVLMA: global validation of linear model assumptions

NND: nearest neighbour distance

PE: mean number of all predators per expedition

PS: mean number of all predators per string

SE: mean number of sharks per expedition

SS: mean number of sharks per string

wAIC: Akaike information criterion weight

1 Introduction

1.1 The importance of schooling fishes

Forage fishes such as anchovies (Engraulidae), pilchard (Clupeidae), and scads (Carangidae), function as a trophic link between plankton and large-bodied vertebrates such as fishes, marine mammals and seabirds, and thus play a key role in structuring marine ecosystems [1]. In addition, forage fish are also the targets of commercial fisheries, with over 31.5 million tonnes landed per year, constituting 37 % of the global wild marine fish catch [2]. Most forage fish catches are destined for non-food uses, such as reduction into fishmeal and fish oil to be used in aquaculture and agriculture [1]. Forage fish can experience rapid population increase due to high fecundity (i.e. batch spawning), early maturity and fast growth, but they are sensitive to environmental conditions, as shown by major populations fluctuations in response to climatic events and human exploitation [2].

Forage fish often congregate in large schools of hundreds to thousands of individuals. A school can be defined as a set of individuals presenting a significant degree of cohesion, living in a group and exhibiting synchronised movements in terms of swimming speed and body orientation [3]. Such behaviour is primarily thought to provide a defence mechanism against predation [3], although it makes fish more detectable and easier to catch with modern fishing techniques [4]. Schooling behaviour is also beneficial for foraging [3] and generates energy savings [5], as shown by a decreased tail beat frequency and reduced metabolic rate [6]. Despite schools increasing individual competition for food [3] and hypoxia [5], schooling remains a very common behaviour amongst fishes. The benefits of schooling behaviour, however, are a function of individual placement within the school. Individuals at the leading edge of the school have greater access to resources such as food and oxygen, but are more exposed to predators and benefit less from hydrodynamics. Consequently, fish regularly switch places within the school [5].

1.2 Effects of predator abundance

Predators affect prey populations through lethal and non-lethal effects. These effects are particularly important in ecosystems driven by predation such as the open ocean [7]. Lethal effects represent prey been killed by predators, while non-lethal effects include behavioural modifications to lower predation risk [8]. Non-lethal effects are sometimes neglected, although they also regulate population sizes through indirect ways. Indeed, shark abundance affects the behaviour of marine turtles, dugongs and dolphins [9]. Studies on non-lethal effects have given rise to the “seascape-of-fear” paradigm [8], a marine adaptation of the “landscape-of-fear” paradigm [10], which provides an explanation for changes in prey behaviour in relation to predator abundance.

Numerous marine predator species are declining, including marine mammals, bony fishes and sharks

[11]. This decline in top predators is predicted to result in trophic cascades, benefiting mesopedators but disadvantaging primary consumers [12], although classification in top and mesopredators is artificial and depends on the ecosystem [13]. Much remains to be known about how marine top predators affect preys behaviour, and such knowledge would strongly benefit predictions on effects of marine predator loss by integrating risk effect [11]. Piscivorous sharks are keystone predators which regulate pelagic ecosystems through predation at different levels [12]. Thus a decline in shark populations may result in a decrease in predation pressure on prey populations [11]. Recent studies have confirmed this hypothesis, bringing to light both lethal and non-lethal effects. Indeed it has been shown that shark abundance affects the diversity, abundance, biomass, and size of reef fishes through lethal effects [14], while fish diet and body condition are conditioned by risk effects [15]. These studies have focused on a few demersal fish families such as Lutjanidae, Lethrinidae and Serranidae.

The non-lethal effects of different predator classes (sharks, teleosts, marine mammals, etc.) on pelagic fish behaviour, and particularly schooling behaviour, remain unknown, as well as the consequences of declines in predator populations for pelagic ecosystems. Although studies have been conducted about how fish schools respond to real or simulated predator presence or attack while enclosed in a tank [16, 17] or a net [18], they only focused on the immediate avoidance response or the position of the attacked fish. It is also relevant to consider larger scales of predation pressure. No study to date have investigated forage fish school characteristics in relation to the predator abundance *in situ*.

1.3 Schooling behaviour quantification

Schooling behaviour can be described by a set of quantitative indices, characterising both group cohesion and group polarity [19]. Quantifying group cohesion requires the spatial position of each fish, in a minimum of two but preferably three dimensions. This requires modelling each fish as a finite object defined by a particular point such as the snout or the centre of mass [19]; the choice of this point is crucial as it influences the computations. The characterisation of group polarity requires supplemental data: body axis or direction vector for polarity, deduced from both fork and snout position, and velocity vector for swimming synchronisation [19]. Thus, knowing fish three-dimensional positions and orientations, we can compute a set of indices to characterise wild fish schools and investigate the effects of external factors such as predation pressure. Similarly, quantifying the inner structure of bird flocks has been done with analogous indices characterising both group cohesion and polarity [20].

1.4 Fish school studies

Most investigations of fish schooling behaviour have been carried out *ex situ* in tanks or swimming tunnels. Published studies have explored schooling behaviour adaptations in response to extrinsic parameters

such as flow velocity [21], light [22], turbidity [23], oxygen level [5], predator presence [16], and predator stimulus [17]. The influence of intrinsic factors such as species [24], group size [25], body length [26] and nutritional state [26] has also been documented, as well as the role of the lateral line and visual acuity [27].

In these studies, fish positions are typically described in two dimensions using a single camera set up to provide a top-down view. Such approaches, however, fail to reproduce natural schooling behaviour and, importantly, ignore the vertical plane [26]. Alternative setups designed to describe fish position in three dimensional space have used 45 degrees inclined [28] or vertical [21] mirrors, side-cameras in addition to the top-camera [25], stereo cameras [29], or records of fish shadows given appropriate lighting [29, 24, 27, 16]. These methods are well adapted to describe the inner structure of fish schools as well as immediate responses to controlled conditions, but the number of individuals on which they can be tested remains limited, and fish behaviour might be altered by human handling.

By contrast, field studies routinely rely on multibeam sonars to quantify global school properties such as overall shape or volume. However, active acoustics methods provide very limited information with respect to the internal school structure and does not support species identification. In particular, multibeam sonar cannot be used to readily identify species, and the poorly known acoustics properties of sharks make them difficult to detect by echo-sounding.

Global fish school properties can also be investigated from aerial photography [30], in which the vertical dimension is often neglected. This approach is not limited to schooling forage fish, and has been used, for instance, to investigate the behaviour of seal herds under high predation risk by sharks [31]. As a compromise between *in* and *ex situ* studies, enclosing nets and echo-sounders have been used to quantify the three-dimensional position of fish in relation to simulated predator attacks [18].

1.5 Underwater baited videography

Here we proposed a novel approach to the study of schooling forage fish based on underwater baited stereo-videography. This method allows extraction of fish position in three dimensions in wild fish schools. Similar methods of stereo-photography and stereo-videography have been developed to study the inner structure of *in situ* bird flocks in three dimensions [20]. Underwater baited videography is an accurate, non-lethal and cost-effective way to study marine species, particularly applicable to environments inaccessible to SCUBA divers [32, 33]. Unlike standard videography, baited video systems actively attract wildlife to the camera field of view to maximise the detection of a large suite of often elusive species but does not bias the relative abundance of trophic classes [34].

This technique has been shown to survey greater intraspecific and interspecific diversity than other methods such as unbaited stationary video systems, diver operated video transects, or fish traps [34]. Mid-

water baited remote underwater stereo-video systems (stereo-BRUVS) are an adaptation of baited videography that allow quantitative measurements of body length and three-dimensional position in the pelagic environment [32, 33]. This method, by allowing collection of fish three-dimensional position, is thus well adapted to study the inner structure of wild fish schools.

1.6 *Decapterus*: the model taxon

Here we present an application of three-dimensional quantification based on stereo-videography to study the schooling behaviour of scads (*Decapterus* sp.) in response to predator abundance. Scads were selected as the focal taxon as they are small pelagic fish vulnerable to numerous species of predators (**Figure 1**). They display schooling behaviour and have been observed on video across a range of locations that varied in predator abundance. The *Decapterus* genus includes 10 species, representing a range of size between 10 and 30 cm for mature individuals and can be hard to identify at the species level on video. The different species of *Decapterus* are found worldwide and, according to the FAO, they represent the eighth most important catch in 2014, with nearly 1.5 million tonnes landed. Scads are thus well adapted for a case study of the effects of predator abundance on schooling behaviour.

Figure 1 – Subpart of a *Decapterus* sp. school, the model taxon used in this study as schooling forage fish.

Using data from diverse locations, we explore the three-dimensional effects of predator abundance on forage fish using *Decapterus* as a model system. Our working hypothesis is that higher predation risk leads to denser fish schools. This work provides key information on the adaptations of fish schooling behaviour to predation pressure at a range of spatial scales, following on the recommendations of [35] that studies of risk effects (1) incorporate multiple scales, (2) consider ”true” or background predation risk and (3) evaluate multiple competing hypotheses.

2 Material and methods

2.1 Video recording with mid-water BRUVS

Baited remote underwater stereo-video systems (stereo-BRUVS) are a non-lethal sampling method for underwater ecosystems. Originally developed for deployment on the seabed, they have been modified to

sample pelagic species in the mid-water environment [32, 33, 36]. Mid-water stereo-BRUVS consists of two GoPro cameras placed on a horizontal base bar, separated by 80 cm and converging inwardly at an angle of 4 degrees. The fields of view from both cameras thus overlap, which allows fish body lengths to be measured and the positions of individuals in three-dimensional space to be determined using epipolar geometry. A horizontal bait arm (180 cm) is placed perpendicularly to the base bar, carrying a bait canister made of a 45 cm long perforated PVC pipe filled with 1.5 kg of fish bait (pilchard or sardine). A weighted vertical rig (160 cm) is placed orthogonally to the two bars and is linked to surface buoys such that the rig is suspended at approximately 10 m (**Figure 2**). Wave-induced motion is limited by using a bungee cord that acts as a shock absorber. BRUVS are typically set in "strings" of 5 replicates separated by 200 m across a long line, for a total distance of 800 m. The string is not anchored and drifts for two hours [33]. Each string is fitted with a flag as well as a GPS tracking unit or a VHF transponder to follow its position. Drop and pick-up coordinates and time are registered for each BRUVS.

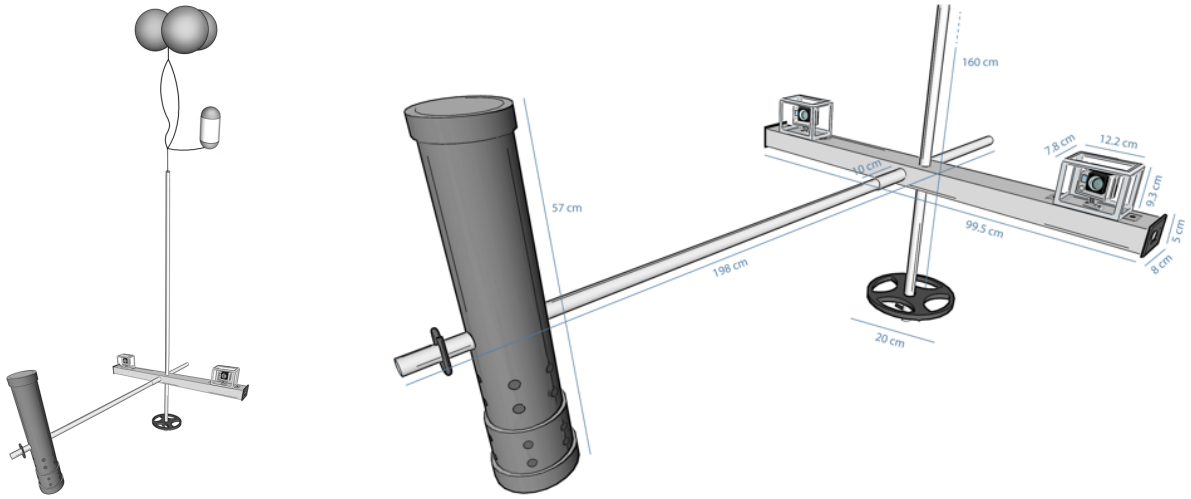

(a) **(b)**

Figure 2 – Schematic representation of a stereo-BRUVS, full view **(a)** and dimensions **(b)**.
Credits: Centre for Marine Futures.

2.2 Sampling locations

Since 2012, the Marine Futures Lab at the University of Western Australia (www.meeuwig.org) has conducted field expeditions in 39 locations globally, gathering pelagic video footage from approximately 3,500 mid-water BRUVS deployments. The locations span 67 degrees of latitude (-37.9° to 30.1°) and 343 degrees of longitude (-178.5° to 164.8°) and encompass the range of our model taxon. After reviewing the global database, five locations were selected (**Table 1**, **Figure 3**) on the basis that multiple schools (n > 4 individuals) of *Decapterus* sp. were observed across a gradient of predator abundances representative of the variation across sampled locations. We selected six independent schools that varied

in size and that were recorded on six independent longlines at each of Revillagigedo Islands, the British Indian Ocean Territory, the Cocos (Keeling) Islands, Ningaloo Reef and four schools for Palau, for a total sample size of 28 schools.

Table 1 – Description of field expeditions from which samples were selected.

Expedition	Year	Start date	Finish date	Latitude (dd)	Longitude (dd)	N	n
Chagos - PCI* II	2015	10-Jan	24-Jan	− 6.3557	72.4434	260	6
Cocos (Keeling)	2016	13-Nov	11-Dec	−12.1325	96.8366	105	6
Ningaloo	2016	15-Sep	22-Sep	−21.8418	113.5772	79	6
Palau - PS**	2014	2-Sep	22-Sep	7.4299	134.4550	147	4
Revillagigedo - PS**	2016	30-Mar	11-Apr	19.0469	−111.0612	75	6
Total						666	28

* Pangea Chagos Initiative (www.meeuwig.org/projects/pangaea-initiative)
** Pristine Seas (www.nationalgeographic.org/projects/pristine-seas)
dd = decimal degrees, N = number of samples available, n = number of schools selected.

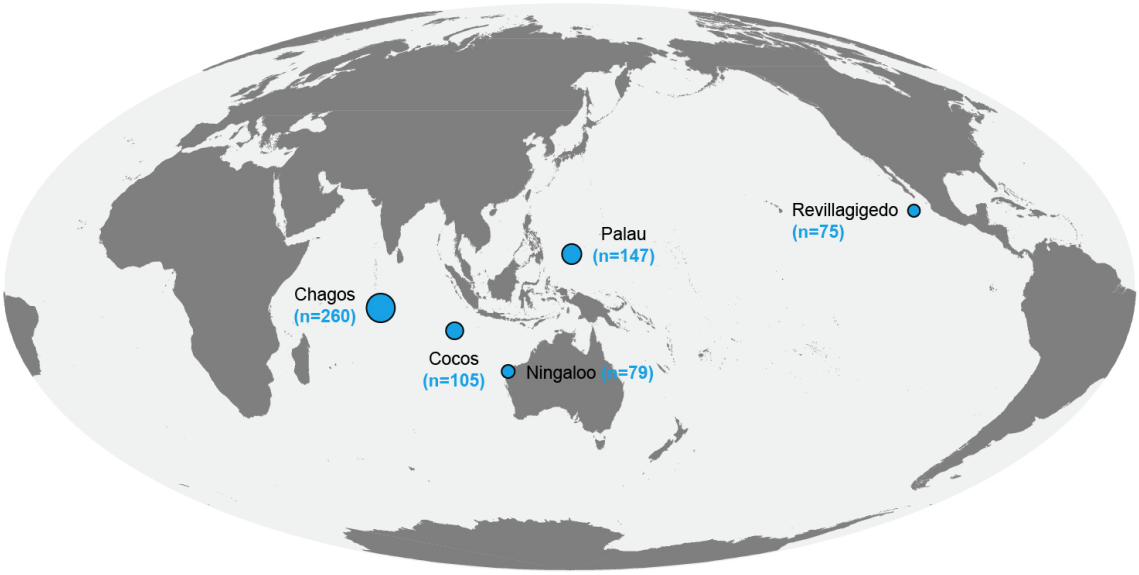

Figure 3 – Map of selected sampling locations. n = number of samples available.

2.3 Metrics from BRUVS

Imagery from the field programme was analysed using the *EventMeasure* software (www.seagis.com.au). Every animal present in recordings was identified to the lowest possible taxonomic level. Relative abundance was estimated as the maximum number (MaxN) of individuals of a given taxon observed in a single frame. Measurements were made where the fish were seen on both cameras simultaneously and no farther than 10 m away from rig. For each school, we selected the frame containing the largest number of *Decapterus* individuals that can be measured, and measured the snout (S) and fork (F) position of each

schooling fish, where possible. Doing so allowed us to obtain the three-dimensional position of every fish, as well as spatial orientation.

Predators were defined as any animal identified on the stereo-BRUVS having a trophic level greater than 4.3 (**Table 2**), which is consistent with known trophic values for carnivorous sharks and bony fish [12]. MaxN was also used as an index of relative abundance, and MaxN values were summed for each sample to obtain an overall predator abundance index. From this, the average predator abundance was calculated per string and per location. We considered two categories of predators, namely (1) sharks only and (2) all predators (**Table 2**) including sharks, teleosts and marine mammals, as these taxa may differentially interact with forage species.

2.4 Computation of school characteristics

For each school, snout and fork positions of each fish in three-dimensional space were used to compute a set of quantitative parameters using *MATLAB R2018a*. These two positions were first used to determine the body axis of each fish. Fish positions were taken to be the point E_p as the approximate projection of eye position on the body axis, located 0.15 fork length (FL) away from the snout. We also defined E_c as the projection of the eye position (E) on the coronal plane (**Figure 4**). Measurements of snout and fork positions could not be completed on every fish because some were hidden by a conspecific, another animal, floating debris, or the bait arm. In such cases, we used E and either S or F positions, assuming that E and E_c coincide, i.e. E belongs to the coronal plane. To do this we defined the angles α and β, respectively $\widehat{E_p S E_c}$ and $\widehat{E_p F E_c}$ (**Figure 4**). Where only S and E were known, body axis was computed using the average value of α of other fish and E_p was placed on the body axis distant of 0.15 FL from S. Where only F and E were known, body axis was computed using the average value of β and E_p was placed on the body axis distant of 0.85 FL from F. The three-dimensional position and orientation of each fish were then used to compute the following set of quantitative indexes for each school: nearest neighbour distances to first (NND1), second (NND2) and third (NND3) neighbour, NND1/NND2 and NND2/NND3 ratios (homogeneity thereafter), mean distance to school centre (expanse thereafter), visible volume, density and polarity index. Each index is described in more detail below.

2.4.1 Nearest neighbours distances

The distance between any given individual and all others can be calculated based on the three-dimensional position of each fish inside a school. The distance D_{ij} between two fish i (x_i, y_i, z_i) and j (x_j, y_j, z_j) in space is given by the formula:

$$D_{ij} = \sqrt{(x_i - x_j)^2 + (y_i - y_j)^2 + (z_i - z_j)^2}$$

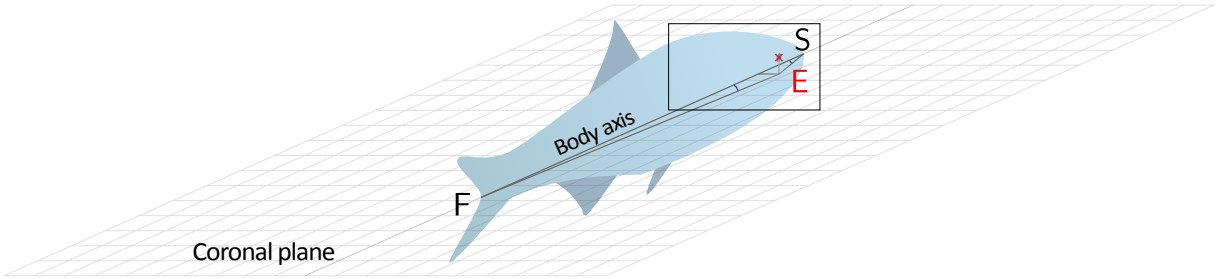

(a)

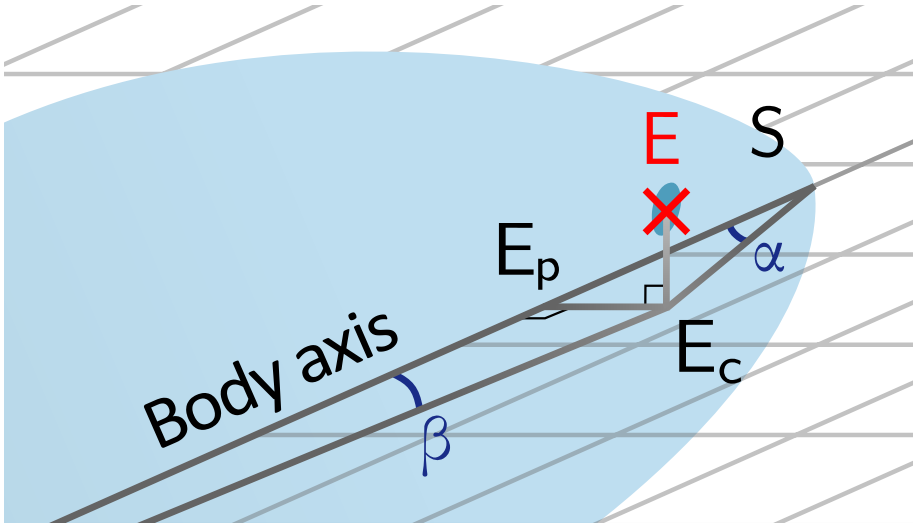

(b)

Figure 4 – Eye position, projection on coronal plane and body axis and definition of angles α and β. Full view **(a)** and zoom at the eye level **(b)**. S = snout, F = fork, E = eye, E_c = projection of eye position on coronal plane, E_p = projection of eye position on body axis.

Table 2 – List of predators and their repartition into predator categories.

Binomial	Common Name	Trophic level*	All predators	Sharks
Acanthocybium solandri	wahoo	4.34	y	n
Carangoides fulvoguttatus	yellowspotted trevally	4.40	y	n
Caranx ignobilis	giant trevally	4.35	y	n
Carcharhinus albimarginatus	silvertip shark	4.35	y	y
Carcharhinus amblyrhynchoides	graceful shark	4.22	n	y
Carcharhinus amblyrhynchos	blacktail reef shark	4.31	y	y
Carcharhinus amboinensis	pigeye shark	4.29	n	y
Carcharhinus brachyurus	copper shark	4.50	y	y
Carcharhinus brevipinna	spinner shark	4.35	y	y
Carcharhinus cautus	nervous shark	4.23	n	y
Carcharhinus falciformis	silky shark	4.46	y	y
Carcharhinus galapagensis	Galapagos shark	4.29	n	y
Carcharhinus leucas	bull shark	4.33	y	y
Carcharhinus limbatus	blacktip shark	4.42	y	y
Carcharhinus longimanus	oceanic whitetip shark	4.28	n	y
Carcharhinus obscurus	dusky shark	4.35	y	y
Carcharhinus plumbeus	sandbar shark	4.36	y	y
Carcharhinus sorrah	spot-tail shark	4.23	n	y
Carcharhinus sp	requiem sharks	4.32	y	y
Carcharhinus tilstoni	Australian blacktip shark	4.37	y	y
Coryphaena equiselis	pompano dolphinfish	4.50	y	n
Coryphaena hippurus	common dolphinfish	4.43	y	n
Delphinus delphis	common dolphin	4.50	y	n
Euthynnus affinis	kawakawa	4.49	y	n
Galeocerdo cuvier	tiger shark	4.48	y	y
Grammatorcynus bicarinatus	shark mackerel	4.50	y	n
Gymnosarda unicolor	dogtooth tuna	4.50	y	n
Istiompax indica	black marlin	4.48	y	n
Istiophoridae sp	billfishes	4.48	y	n
Istiophorus albicans	Atlantic sailfish	4.46	y	n
Istiophorus platypterus	Indo-Pacific sailfish	4.50	y	n
Isurus oxyrinchus	shortfin mako	4.41	y	y
Kajikia audax	striped marlin	4.50	y	n
Lamna nasus	porbeagle	4.47	y	y
Makaira mazara	Indo-Pacific blue marlin	4.46	y	n
Makaira nigricans	blue marlin	4.44	y	n
Mesoplodon densirostris	Blainville's beaked whale	4.38	y	n
Orcinus orca	killer whale	4.60	y	n
Prionace glauca	blue shark	4.36	y	y
Pseudorca crassidens	false killer whale	4.50	y	n
Rhizoprionodon acutus	milk shark	4.17	n	y
Scomberoides tol	needlescaled queenfish	4.31	y	n
Scomberomorus commerson	narrow-barred Spanish mackerel	4.44	y	n
Scomberomorus munroi	Australian spotted mackerel	4.32	y	n
Scomberomorus sp	Spanish mackerels	4.36	y	n
Seriola hippos	samson fish	4.32	y	n
Seriola rivoliana	longfin yellowtail	4.48	y	n
Seriola sp	amberjacks	4.32	y	n
Sphyraena barracuda	great barracuda	4.50	y	n
Sphyraena jello	pickhandle barracuda	4.50	y	n
Sphyraena sp	barracudas	4.32	y	n
Sphyrna lewini	scalloped hammerhead	4.15	n	y
Sphyrna mokarran	great hammerhead	4.38	y	y
Sphyrna sp	hammerheads	4.24	n	y
Sphyrna zygaena	smoooth hammerhead	4.32	y	y
Stenella attenuata	pantropical spotted dolphin	4.47	y	n
Stenella frontalis	Atlantic spotted dolphin	4.50	y	n
Stenella sp	oceanic dolphin	4.50	y	n
Tasmacetus shepherdi	Shepherd's beaked whale	4.50	y	n
Thunnus albacares	yellowfin tuna	4.45	y	n
Thunnus obesus	bigeye tuna	4.49	y	n
Tursiops truncatus	bottlenose dolphin	4.50	y	n
Ziphiidae sp	beaked whales	4.50	y	n

*Trophic levels were found on FishBase (www.fishbase.org) for fishes and on SeaLifeBase (www.sealifebase.org) for other taxa. For unidentified species, trophic level was taken as the genus mean trophic level.

From the interdistance between each fish in the school, the mean nearest neighbour distance ($\overline{NND}$) was computed as:

$$\overline{NND} = \frac{1}{n} \sum_{i=1}^{n} \min_{i \neq j} D_{ij}$$

Similar computation was done for second and third neighbours. All these distances were expressed as a function of the mean FL of the considered school to allow comparison between schools [19].

2.4.2 Homogeneity

To assess school structure homogeneity, we calculated the NND_1/NND_2 and NND_2/NND_3 ratios. The closer these ratios are to one, the more regularly the school is structured locally [19].

2.4.3 School expanse

Average distance to the centre of gravity *C* of the school was computed as an index of the group expanse ϵ. *C* coordinates (x_C, y_C, z_C) were respectively calculated as the average of x, y and z values [19].

$$\epsilon = \frac{1}{n} \sum_{i=1}^{n} \sqrt{(x_i - x_C)^2 + (y_i - y_C)^2 + (z_i - z_C)^2}$$

$$\text{with} \quad x_C = \frac{1}{n} \sum_{j=1}^{n} x_j \quad ; \quad y_C = \frac{1}{n} \sum_{j=1}^{n} y_j \quad \text{and} \quad z_C = \frac{1}{n} \sum_{j=1}^{n} z_j$$

This metrics is also standardised for the mean for length of the school.

2.4.4 Visible school volume

We used two methods to calculate the volume occupied by a group of fish: the convex hull and the alpha shape. A convex hull is the minimal convex envelope containing an entire point cloud, while alpha shapes account for concavities of a given radius [20]. For the later, radii were chosen such that the computed volume equalled the volume of the smallest polyhedron containing all the individuals. Accordingly, convex hulls give an upper estimate of the volume while alpha shapes give a lower estimate, and conversely for density. Because we are likely to work on schools subparts, we could only compute a visible volume, which is not indicative of the global school volume. Thus, this piece of information cannot be used to draw conclusions about the whole school size, but reported to the number of fish it provides a measurement of the school packing. In any case, the volume was expressed as a cubic function of the mean FL for the considered school to standardise for variation in fish size.

2.4.5 School density

With the number of individuals in a visible school volume, a local density was estimated as a number of individuals per volume, expressed in FL^{-3} such that it is standardised. Assuming that the school is homogeneous, global school density can be considered equal to local density.

2.4.6 Polarity index

For each fish, body direction was computed from the body axis vector, deduced from snout and fork position, the norm of this vector being the FL. After standardisation (norm = 1), a mean vector representing the direction toward which the school is moving was calculated. The group polarity Φ is the mean angle deviation between the group mean vector ($\vec{GV}$) and each fish vector ($\vec{f_i}$) in three-dimensional space.

$$\Phi = \frac{1}{n} \sum_{i=1}^{n} \arccos \frac{\vec{GV} \cdot \vec{f_i}}{\|\vec{GV}\| \times \|\vec{f_i}\|}$$

This value is comprised between 0 (high polarity) and $\pi/2$ (no polarity). Φ was converted to a non-dimensionalised variable defined by $\Phi^* = (\frac{\pi}{2} - \Phi)/\frac{\pi}{2}$. Thus Φ^* is an index between 0 (no polarity) and 1 (high polarity) [25].

2.5 Statistical analysis

To asses whether fish schools are tighter in areas with higher predator abundance, we built linear regression models to describe fish school attributes as a function of eight explanatory variables reflecting competing hypothesises [35]. The first four explanatory variables relate to predator abundance and allow us to test our core hypothesis on the influence of predation risk: all predators per string, all predators per expedition, sharks per string and sharks per expedition. We also included four variables to control for variability in the inherent attributes of the schools: number of fish, mean fork length; and the proportions of fish on the border of the school for the convex hull and alpha shape estimates (**Table 3**). We used combinations of these predictors to build 39 linear regression models containing between one and three explanatory variables which are not correlated (absolute value of Spearman's r < 0.6) (**Table 4**) in order to predict school attributes. Models were then ranked based on their Akaike information criterion (AIC) scores, obtained from the *MuMIn* package in *R 3.4.3*. Models with a Δ(AIC) value higher than 2 were rejected, and AIC weights (wAIC) were recomputed based on this subset. All models were checked for meeting global validation of linear model assumptions (GVLMA) with a level of significance of 5%, using the *R gvlma* package, and models which did not meet these assumptions were rejected. Variance partitioning analysis was done with the *R vegan* package. Volume and density values were converted to decimal logarithm to reduce skewness given the large range of values observed. All variables were

standardised by subtracting the mean and dividing by two standard deviations.

3 Results

3.1 Predictors

We assessed 28 schools from six locations, varying in size from 6 to 51 individuals, with a mean fork length range between 20 cm and 34 cm (**Table 3**).

Of the eight predictor variables, the proportion of fish on the school border for the convex hull was positively correlated with that for the alpha shape (Spearman's $r = 0.67$, $p < 0.001$). These two variables were also negatively correlated with the number of fish in the school ($r = -0.87$, $p < 0.01$ and $r = -0.65$, $p < 0.01$ respectively). Predator and shark abundance were strongly correlated, both at the string (Spearman's $r = 0.80$, $p < 0.01$) and expedition level ($r = 1.00$, $p < 0.001$). Measures of shark abundance were correlated at both the expedition and the string level ($r = 0.70$, $p < 0.01$), as was predator abundance ($r = 0.81$, $p < 0.01$) (**Table 4**). This result shows that predator and shark abundance are consistent between the string and the expedition level. All of the other 19 combinations of predictors were not correlated with Spearman's r between -0.6 and 0.6 (**Table 4**).

Table 3 – Summary of raw explanatory and response variables used in models of fish school attributes.

Variable	Units	Abbrev.	Min	Med	Mean	Max	Std
Predators							
Mean number of sharks per string	1	SS	0.00	0.00	0.57	4.00	1.04
Mean number of sharks per expedition	1	SE	0.01	0.46	0.62	1.63	0.59
Mean number of all predators per string	1	PS	0.00	0.30	1.70	20.33	4.05
Mean number of all predators per expedition	1	PE	0.11	0.57	1.44	4.67	1.76
School attributes for standardisation							
Number of fish per school	1	FN	6.00	14.50	19.71	51.00	13.15
Mean fork length of fish per school	cm	FL	0.02	0.07	0.09	0.34	0.06
Proportion of fish on border of alpha shape	1	BFAS	0.81	1.00	0.97	1.00	0.05
Proportion of fish on border of convex hull	1	BFCH	0.40	0.72	0.71	1.00	0.18
School attributes to be predicted							
Mean distance to closest 1st neighbour*	FL	NND1	1.30	2.15	2.34	4.43	0.89
Mean distance to closest 2nd neighbour*	FL	NND2	1.75	3.01	3.13	6.64	1.28
Mean distance to closest 3rd neighbour*	FL	NND3	2.11	3.49	3.79	8.20	1.59
Mean distance to the school centre (expanse)*	FL	Exp	1.67	4.00	4.78	11.99	2.47
School volume based on alpha shape*†	FL^3	VolAS	1.61	51.83	192.24	901.59	258.85
School volume based on convex hull*†	FL^3	VolCH	2.03	92.46	409.23	1967.10	607.30
Fish density based on alpha shape*†	FL^{-3}	DenAS	0.03	0.26	0.57	4.35	0.89
Fish density based on convex hull*†	FL^{-3}	DenCH	0.01	0.15	0.37	3.45	0.66
Mean deviation angle to the school direction‡	1	Pol	0.26	0.77	0.72	0.91	0.17
Homogeneity between 1st and 2nd nearest neighbour distance	1	Hom12	0.55	0.78	0.76	0.88	0.07
Homogeneity between 2nd and 3rd nearest neighbour distance	1	Hom23	0.45	0.64	0.64	0.72	0.06

* standardised for fork length

† converted to decimal logarithm

‡ non-dimensional variable between 0 (no polarity) and 1 (high polarity)

Table 4 – Spearman's *r* values for predictor correlations.

	FN	FL	BFCH	BFAS	PS	SS	PE	SE
FN	1.00							
FL	**−0.34**	1.00						
BFCH	−0.87	**0.29**	1.00					
BFAS	−0.65	**0.27**	0.67	1.00				
PS	**0.00**	**−0.24**	**−0.02**	**0.14**	1.00			
SS	**0.05**	**−0.31**	**0.00**	**0.08**	0.80	1.00		
PE	**0.07**	**−0.09**	**−0.02**	**0.24**	0.81	0.70	1.00	
SE	**0.07**	**−0.09**	**−0.02**	**0.24**	0.81	0.70	1.00	1.00

Values between −0.6 and 0.6 are in bold. Acronyms are spelled out in **Table 3**.

Table 5 – Equations of the best model for each school attribute for which an appropriate model was found.

Metric	Equation	R^2	R^2_{pred}	*wAIC*	*ER*
NND1	$= 0.69\ (0.14) \cdot \text{SE}^{**}$	48.0%	48.0%	1.000	–
Hom23	$= -\ 0.40\ (0.18) \cdot \text{BFCH}^{*}$	15.7%	0%	0.434	1.28
Exp	$= 0.57\ (0.13) \cdot \text{SE}^{**} + 0.50\ (0.13) \cdot \text{FN}^{**}$	54.6%	31.4%	0.506	1.91
log (VolCH)	$= 0.51\ (0.10) \cdot \text{PE}^{**} + 0.76\ (0.10) \cdot \text{FN}^{**}$	75.8%	25.9%	0.432	1.05
log (VolAS)	$= 0.51\ (0.10) \cdot \text{SE}^{**} + 0.72\ (0.10) \cdot \text{FN}^{**}$	75.3%	25.7%	0.455	1.24
log (DenCH)	$= -\ 0.62\ (0.12) \cdot \text{SE}^{**} - 0.51\ (0.12) \cdot \text{FN}^{**}$	62.7%	38.7%	0.388	1.17
log (DenAS)	$= -\ 0.62\ (0.13) \cdot \text{SE}^{**} - 0.48\ (0.13) \cdot \text{FN}^{**}$	59.7%	38.7%	0.644	1.81

* p-value < 0.05, ** p-value < 0.01. Metric acronyms are spelled out in **Table 3**.
R^2_{pred} = variance explained by predator abundance, *wAIC* = AIC weight, *ER* = evidence ratio of the best model compared to the second best model. All models in this table met the global validation of linear models assumptions.

3.2 Effects of predator abundance on school structure

3.2.1 Nearest neighbour distances

One model was selected for NND1, including only SE. This model explained 48.0% of the variance (**Table 5, Figure 5**). In this model, the parameter associated with SE was positive ($p < 0.01$), thus NND1 was bigger in areas with higher predator abundances.

The models selected by AIC for NND2 and NND3 did not meet the GVLMA (**Table 6**) and were thus rejected.

3.2.2 Homogeneity

Of the ten models selected by AIC for Hom12, none met the GVLMA (**Table 6**).

Three models were considered for Hom23. The best model only included BFCH, explained 15.7% of the variance ($p = 0.037$) and had a *wAIC* value of 0.434 (**Table 5**). The two other models included BFCH and a predator attribute, SE or PE. These models respectively explained 22.2% and 19.9% of the variance, and had relatively similar support from the data as shown by the *wAIC* values: 0.339 for the model with BFCH and SE, 0.227 for the model with BFCH and PE (**Table 6**). However, in both models the parameter associated with the predator attribute was not significant ($p = 0.161$ for SE and $p = 0.262$ for PE).

Thus we could not find a relation between homogeneity of interdistances and predator abundance.

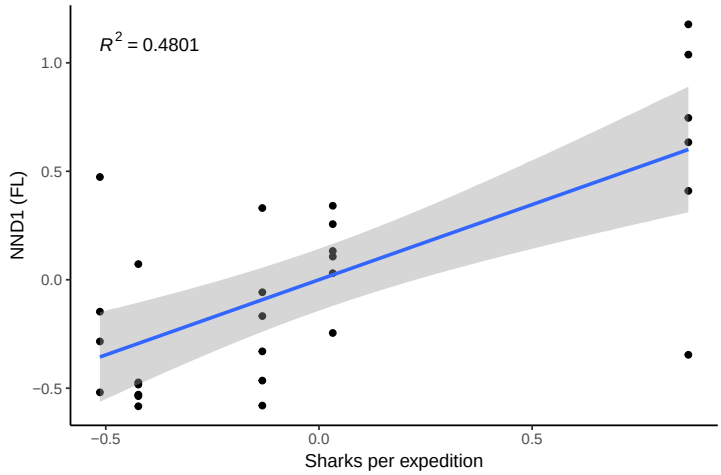

Figure 5 – Linear regression of distance to first nearest neighbour (NND1) against sharks per expedition (SE). 95% confidence interval is shown in grey.

3.2.3 School expanse

Three models were selected for school expanse. The best model included SE and FN, explained 54.6% of the variance ($p < 0.01$) and had a *wAIC* value of 0.506 (**Table 5**), making this model twice more likely than the two other ones. The two other models (SE + BFCH and PE + FN) explained a little less variance (R^2 = 52.4% and 51.9% respectively) and had similar *wAIC* values (0.265 and 0.229 respectively) (**Table 6**). In all models, predator attributes explained more variance than intrinsic fish school attributes. In the best model, including SE and FN, SE explained 31.4% of the variance (**Table 5**). Variance partitioning was similar for the two other models.

The parameter associated with FN was positive (**Table 5**), showing that distance to school centre increases with FN, as expected. In all models, the parameter associated with predator abundance was positive, thus distance to school centre increases with predator abundance.

3.2.4 Visible school volume

Three models were selected for each computation of visible school volume.

For the convex hull computation, the best model included PE and FN. It explained 75.8% ($p < 0.01$) of the variance and had a *wAIC* value of 0.432. The best model for the alpha shape computation included SE and FN, it explained 75.3% ($p < 0.01$) of the variance and had a *wAIC* value of 0.455 (**Table 5**). These two models are as likely as the second ones (SE and FN for VolCH, PE and FN for VolAS), as shown by the similar *wAIC* values (**Table 6**). For both computation, FN explained more variance than the predator attribute (25.9% of variance explained by PE for convex hull and 25.7% explained by SE for alpha shape) (**Table 5**).

The parameter associated with FN was positive ($p < 0.01$), showing that visible volume increased with

FN, as expected. The parameter associated with SE was also positive ($p < 0.01$), thus visible volume increased with predator abundance.

3.2.5 School density

Three models were selected for density computed by convex hull and two models were selected for the alpha shape computation. The best model for DenCH included SE and FN. It explained 62.7% of the observed variance ($p < 0.01$) and had a *wAIC* value of 0.388 (**Table 5**). Thus this model is slightly more likely than the two other ones, which were SE + BFCH and PE + FN, with respective *wAIC* values of 0.332 and 0.280 (**Table 6**). In all models, the predator attribute (SE or PE) explained more variance than the other parameter (38.7% of variance explained by SE in the best model including SE and FN) (**Table 5**). In the best model, the parameters associated with FN and SE were both negative ($p < 0.01$ for both parameters). Thus density computed by convex hull decreased with FN and with predator abundance.
Concerning density computed by alpha shape, the best model included SE and FN (**Table 5**). This model explained 59.7% ($p < 0.01$) of the variance and had a *wAIC* value of 0.644, making it twice more likely than the second model, which included PE and FN, explained 58.0% ($p < 0.01$) of the variance, and had a *wAIC* value of 0.356 (**Table 6**). In both models, predator attribute explained more variance than FN (38.7% of variance explained by SE in the best model including SE and FN) (**Table 5**). Still in this model, the parameters associated with FN and SE were both negative ($p < 0.01$ for both parameters). Thus, for both computation, density decreased with both FN and predator abundance.

3.2.6 Polarity index

The models selected by AIC for polarity index did not meet the GVLMA (**Table 6**) and were thus rejected.

4 Discussion

4.1 Predator abundance affects schooling behaviour

We found that predator abundance changes forage fish schooling behaviour such that school size generally increased with increasing numbers of predators. NND1, expanse and visible volume all increased with predator abundance while density decreased. This result was unexpected because it has often been proposed that higher predation risk will make schools more compact [37]. The exception was homogeneity that did not seem to be affected by predator abundance. Moreover, none of the model that we built was appropriate to explain the variation in school polarity.
Possible explanations are that predation pressure is not important enough to force fish to school in a tighter way, and that schooling behaviour is driven by other environmental factors. One factor known

Table 6 – All models selected by AIC.

Metric	Model	Explanatory Variables	R^2	*wAIC*	$wAIC/wAIC_{best}$	GVLMA
NND1	Model 1	SE**	48.0%	1.000	1.000	y
NND2	Model 1	SE**	30.0%	0.477	1.000	n
	Model 2	PE**	28.4%	0.347	0.727	n
	Model 3	SE**, BFAS	31.8%	0.176	0.369	n
NND3	Model 1	SE**	30.8%	0.335	1.000	n
	Model 2	PE**	29.3%	0.248	0.740	n
	Model 3	SE**, BFAS	33.3%	0.145	0.433	n
	Model 4	SE**, BFCH	33.2%	0.140	0.418	n
	Model 5	SE**, FN	32.9%	0.133	0.397	n
Hom12	Model 1	SE	6.5%	0.199	1.000	n
	Model 2	PE	3.8%	0.134	0.673	n
	Model 3	SS	3.2%	0.122	0.613	n
	Model 4	FL	2.1%	0.105	0.528	n
	Model 5	PS	1.4%	0.095	0.477	n
	Model 6	BFCH	1.2%	0.092	0.462	n
	Model 7	FN	0.7%	0.087	0.437	n
	Model 8	SE, FL	9.8%	0.085	0.427	n
	Model 9	BFAS	0.3%	0.082	0.412	n
Hom23	Model 1	BFCH*	15.7%	0.434	1.000	y
	Model 2	SE, BFCH*	22.2%	0.339	0.781	y
	Model 3	PE, BFCH*	19.9%	0.227	0.523	y
Exp	Model 1	SE**, FN**	54.6%	0.506	1.000	y
	Model 2	SE**, BFCH**	52.4%	0.265	0.524	y
	Model 3	PE**, FN**	51.9%	0.229	0.453	y
log (VolCH)	Model 1	PE**, FN**	75.8%	0.432	1.000	y
	Model 2	SE**, FN**	75.7%	0.404	0.935	y
	Model 3	PE**, FN**, BL	76.7%	0.165	0.382	y
log (VolAS)	Model 1	SE**, FN**	75.3%	0.455	1.000	y
	Model 2	PE**, FN**	74.9%	0.368	0.809	y
	Model 3	PE**, FN**, BL	76.2%	0.177	0.389	y
log (DenCH)	Model 1	SE**, FN**	62.7%	0.388	1.000	y
	Model 2	SE**, BFCH**	62.3%	0.332	0.856	y
	Model 3	PE**, FN**	61.8%	0.280	0.722	y
log (DenAS)	Model 1	SE**, FN**	59.7%	0.644	1.000	y
	Model 2	PE**, FN**	58.0%	0.356	0.499	y
Pol	Model 1	PS*	19.6%	0.667	1.000	n
	Model 2	BFAS, PS*	23.3%	0.333	0.499	n

* p-value < 0.05, ** p-value < 0.01. Metric acronyms are spelled out in **Table 3**.
wAIC = AIC weight, GVLMA = global validation of linear model assumptions.

to affect fish schooling behaviour is oxygen level. *Ex situ* studies have shown that school exposed to hypoxia are less packed, as shown by increased length, area and volume, until school disruption [5], but these results vary among species. These effects are exacerbated in a school, where oxygen level is decreasing because of fish's consumption [5]. This could explain why we found that density decreases with fish number. In the light of oxygen effect, one hypothesis to explain our result is that fish maintain higher distances between each other in areas with a higher predation risk, increasing the available volume per fish so that each fish have access to a bigger oxygen reserve if needed. Indeed, according to the gill oxygen limitation theory [38], fish are already on the high limit of oxygen consumption. Thus, schooling fish have access to less oxygen than non schooling fish, but this is counter-balanced by energy savings provided by schooling behaviour. However, this limit in oxygen availability turns out to be a limit for metabolism, and a sudden need for oxygen, to escape from a predator for example, might not be covered by the available oxygen, leading to an oxygen debt. Hence, looser schools might be an appropriate way to ensure escaping ability for schooling fish under higher predation pressure.

All metrics of predators showed very similar results, regardless if all predators or sharks only where included, although models including sharks instead of all predators often had better AIC rankings. For all the selected models including a predator attribute, this predator attribute was always computed at the expedition level, showing that global predator abundance is more relevant.

All metrics except NND1 had to be controlled for fish attributes. As expected, visible volume and expanse increase with the number of fish in the school. For NND2 and NND3, one of the selected models included the proportion of fish on the border of the alpha shape, although the parameter was not significant. Fish on the border of the school tend to have higher values of NND as they have less neighbours than inner fish. Thus, the mean NND in the school is expected to increase when the proportion of border fish increases. All selected models for density included fish attributes, either fish number or proportion of border fish in the convex hull or alpha shape. Density was negatively correlated with the number of fish in the school and positively correlated with the proportion of border fish. This last point is not surprising as fish number and proportion of border fish were negatively correlated. Thus, density tends to decrease as the number of fish in the school increases.

4.2 BRUVS

BRUVS were shown to be successful to study fish schools *in situ* in a non-invasive way. To our knowledge, this is the first time that wild pelagic fish schools are characterised quantitatively using metrics from the positions of individual fish in three-dimensional space, as captured on stereo-video. Previous attempts to study wild marine fish schools using underwater footage have been made, but they involved only one camera and assumptions around fish body size [37], which is a potential source of imprecision.

4.3 Metrics and challenges

In this study, school volume was computed as both a convex hull and an alpha shape. The convex hull is easier to compute but does not take into account concavities in the group. Volume might thus be over-estimated and the density under-estimated. The alpha shape, which takes concavities into account, is more precise. However there is no absolute way to calculate the non-convex border of a cloud point, and the radius *R* of the concavities that are removed from the convex hull has to be arbitrarily set. If this radius is too high, the shape will converge to the convex hull, and if the radius is too low the set of points may be split into several non-convex shapes. When working on a large set of points, the radius can be set by checking the size of aggregation concavities, which is done by plotting the aggregation density as a function of *R* [20]. However, working with schools containing relatively few fish (FN = 6-51, **Table 3**) precludes such an approach. Instead, we first computed a list of the different radius values which result in different alpha shapes, and then used trial and error to find the appropriate value of *R* which returned the smallest envelope corresponding to one polyhedron. However, this method may require a long computation time if used for large groups (FN > 100). Alpha shapes are particularly adapted for non-convex school shapes such as tori, for which a convex hull modelling would lead to a disc, with a bigger volume than the torus. They are mostly used for bird flocks containing hundreds of individuals and susceptible to displaying concavities.

Here, both methods show very similar results in terms of explained variance and parameters for visible school volume. For density, both computations do not return the same best model, but all selected models have close values of wAIC and are within the same range of explained variance. Thus convex hull and alpha shape computations produce very similar results in our study.

4.4 Limits of the study

Fish schooling behaviour might also be affected by other environmental factors, as demonstrated in many *ex situ* studies. All BRUVS surveys have been carried out during day light, and although luminosity may vary due to weather conditions, these variations are likely not sufficient to affect schooling behaviour [22]. Possible variation in turbidity between days and surveys might affect schooling behaviour [23]. Similarly, current intensity can affect schooling behaviour [21]. Carbone dioxyde level and pH variations have not been documented to affect school structure *ex situ* [5]. To our knowledge, the effects of salinity on schooling behaviour are yet to be explored.

Terrestrial predators are usually classified in apex predators, i.e. large animals occupying the highest trophic level and structuring food webs by affecting lower level organisms via predation and behavioural changes. However this classification is quite artificial, since a species can be an apex predator in an ecosystem and a mesopredator in another ecosystem with larger predators [13]. Predator classification

in marine ecosystems is also affected by this bias, and numerous sharks classified as apex predators on coral reefs actually act as mesopredators, along with large-bodied teleosts [13, 12]. Moreover, such classification for sharks in marine ecosystems should also take into account size of individuals and life stage as these factors influence trophic level [39]. Defining such predator's role in the open ocean is even a harder task due to the lack of sampling in this remote biome.

4.5 Conclusion

This work brings to light the effects of predator abundance on forage fish schooling behaviour. Such information is crucial in a context of declining predators and overexploitation of forage fish which are a major link between low and high trophic levels.

Further investigations should be conducted to confirm these results across a wider range of predator abundances. Studies on schooling behaviour related to *in situ* oxygen level would also be needed to confirm our hypothesis.

References

[1] Pikitch EK, Rountos KJ, Essington TE, Santora C, Pauly D, Watson RA, Sumaila UR, Boersma PD, Boyd IL, Conover DO, Cury P, Heppell SS, Houde ED, Mangel M, Plagányi É, Sainsbury K, Steneck RS, Geers TM, Gownaris N and Munch SB (2014). The global contribution of forage fish to marine fisheries and ecosystems. *Fish Fish.* 15(1): 43–64.

[2] Alder J, Campbell B, Karpouzi V, Kaschner K and Pauly D (2008). Forage Fish: From Ecosystems to Markets. *Annu. Rev. Environ. Resour.* 33(1): 153–166.

[3] Pitcher TJ (1992). *Behaviour of Teleost Fishes*. Chapman and Hall.

[4] Pitcher TJ (1995). The impact of pelagic fish behaviour on fisheries. *Sci. Mar.* 59(3-4): 295–306.

[5] Domenici P, Steffensen JF and Marras S (2017). The effect of hypoxia on fish schooling. *Philos. Trans. R. Soc. London B Biol. Sci.* 372(1727).

[6] Marras S, Killen SS, Lindström J, McKenzie DJ, Steffensen JF and Domenici P (2015). Fish swimming in schools save energy regardless of their spatial position. *Behav. Ecol. Sociobiol.* 69(2): 219–226.

[7] Baum JK and Worm B (2009). Cascading predator and effects of changing oceanic. *Anim. Ecol.* 78(4): 699–714.

[8] Wirsing AJ, Heithaus MR, Frid A and Dill LM (2008). Seascapes of fear: evaluating sublethal predator effects experienced and generated by marine mammals. *Mar. Mammal Sci.* 24(1): 1–15.

[9] Heithaus MR, Wirsing AJ and Dill LM (2012). The ecological importance of intact top-predator populations: a synthesis of 15 years of research in a seagrass ecosystem. *Mar. Freshw. Res.* 63(11): 1039–1050.

[10] Laundré JW, Hernández L and Altendorf KB (2001). Wolves, elk, and bison: reestablishing the ”landscape of fear” in Yellowstone National Park, U.S.A. *Can. J. Zool.* 79(8): 1401–1409.

[11] Heithaus MR, Frid A, Wirsing AJ and Worm B (2008). Predicting ecological consequences of marine top predator declines. *Trends Ecol. Evol.* 23(4): 202–210.

[12] Roff G, Doropoulos C, Rogers A, Bozec YM, Krueck NC, Aurellado E, Priest M, Birrell C and Mumby PJ (2016). The Ecological Role of Sharks on Coral Reefs. *Trends Ecol. Evol.* 31(5): 395–407.

[13] Frisch AJ, Ireland M, Rizzari JR, Lönnstedt OM, Magnenat KA, Mirbach CE and Hobbs JPA (2016). Reassessing the trophic role of reef sharks as apex predators on coral reefs. *Coral Reefs* 35(2): 459–472.

[14] Barley SC, Meekan MG and Meeuwig JJ (2017). Diet and condition of mesopredators on coral reefs in relation to shark abundance. *PLoS One* 12(4): e0165113.

[15] Barley SC, Meekan MG and Meeuwig JJ (2017). Species diversity, abundance, biomass, size and trophic structure of fish assemblages on coral reefs in relation to shark abundance. *Mar. Ecol. Prog. Ser.* 565: 1–19.

[16] Abrahams MV and Colgan PW (1985). Risk of predation, hydrodynamic effeciency and their influence on school structure. *Environ. Biol. Fishes* 13(3): 195–202.

[17] Miller N and Gerlai R (2007). Quantification of shoaling behaviour in zebrafish (Danio rerio). *Behav. Brain Res.* 184(2): 157–166.

[18] Rieucau G, De Robertis A, Boswell KM and Handegard NO (2014). School density affects the strength of collective avoidance responses in wild-caught Atlantic herring Clupea harengus: a simulated predator encounter experiment. *J. Fish Biol.* 85: 1650–1664.

[19] Delcourt J and Poncin P (2012). Shoals and schools: back to the heuristic definitions and quantitative references. *Rev. Fish Biol. Fish.* 22(3): 595–619.

[20] Cavagna A, Giardina I, Orlandi A, Parisi G and Procaccini A (2008). The STARFLAG handbook on collective animal behaviour: Part II, three-dimensional analysis. *Anim. Behav.* 76: 237–248.

[21] Pitcher TJ (1973). The three-dimensional structure of schools in the minnow, Phoxinus phoxinus (L.). *Anim. Behav.* 21(4): 673–686.

[22] Glass CW, Wardle CS and Mojsiewicz WR (1986). A light intensity threshold for schooling in the Atlantic mackerel, Scomber scombrus. *J. Fish Biol.* 29(Supplement A): 71–81.

[23] Borner KK, Krause S, Mehner T, Uusi-Heikkilä S, Ramnarine IW and Krause J (2015). Turbidity affects social dynamics in Trinidadian guppies. *Behav. Ecol. Sociobiol.* 69(4): 645–651.

[24] Partridge BL, Pitcher TJ, Cullen JM and Wilson J (1980). The three-dimensional structure of fish schools. *Behav. Ecol. Sociobiol.* 6(4): 277–288.

[25] Viscido SV, Parrish JK and Grünbaum D (2004). Individual behavior and emergent properties of fish schools: a comparison of observation and theory. *Mar. Ecol. Prog. Ser.* 273: 239–249.

[26] Krause J, Reeves P and Hoare D (1998). Positioning Behaviour in Roach Shoals: The Role of Body Length and Nutritional State. *Behaviour* 135(8): 1031–1039.

[27] Partridge BL and Pitcher TJ (1980). The sensory basis of fish schools: Relative roles of lateral line and vision. *J. Comp. Physiol.* 135: 315–325.

[28] Audira G, Sampurna PB, Juniardi S, Liang ST, Lai YH and Hsiao CD (2018). A Simple Setup to Perform 3D Locomotion Tracking in Zebrafish by Using a Single Camera.

[29] Cullen JM, Shaw E and Baldwin HA (1965). Methods for measuring the three-dimensional structure of fish schools. *Anim. Behav.* 13(4): 534–543.

[30] Partridge BL, Johansson J and Kalish J (1983). The structure of schools of giant bluefin tuna in Cape Cod Bay. *Environ. Biol. Fishes* 9(3): 253–262.

[31] De Vos A and O'Riain MJ (2013). Movement in a selfish seal herd: do seals follow simple or complex movement rules? *Behav. Ecol.* 24(1): 190–197.

[32] Letessier TB, Meeuwig JJ, Gollock M, Groves L, Bouchet PJ, Chapuis L, Vianna GMS, Kemp K and Koldewey HJ (2013). Assessing pelagic fish populations: The application of demersal video techniques to the mid-water environment. *Methods Oceanogr.* 8: 41–55.

[33] Bouchet PJ and Meeuwig JJ (2015). Drifting baited stereo-videography: a novel sampling tool for surveying pelagic wildlife in offshore marine reserves. *Ecosphere* 6(8): 1–29.

[34] Coghlan AR, McLean DL, Harvey ES and Langlois TJ (2017). Does fish behaviour bias abundance and length information collected by baited underwater video? *J. Exp. Mar. Bio. Ecol.* 497(Supplement C): 143–151.

[35] Moll RJ, Redilla KM, Mudumba T, Muneza AB, Gray SM, Abade L, Hayward MW, Millspaugh JJ and Montgomery RA (2017). The many faces of fear: a synthesis of the methodological variation in characterizing predation risk. *J. Anim. Ecol.* 86(4): 749–765.

[36] Bouchet PJ, Meeuwig JJ, Huveneers C, Langlois TJ, Lowry M, Rees M, Santana-Garcon J, Scott M, Taylor M, Thompson C, Vigliola L and Whitmarsh S (2018). Marine sampling field manual for pelagic BRUVS (Baited Remote Underwater Videos). In R Przeslawski and S Foster (Editors) *F. Manuals Mar. Sampl. to Monit. Aust. Waters*, pp. 105–132. National Environmental Science Programme (NESP).

[37] Domenici P, Batty RS and Similä T (2000). Spacing of wild schooling herring while encircled by killer whales. *J. Fish Biol.* 57(3): 831–836.

[38] Pauly D and Cheung WWL (2017). Sound physiological knowledge and principles in modeling shrinking of fishes under climate change. *Global Change Biology* 24(1): e15–e26.

[39] Heupel MR, Knip DM, Simpfendorfer CA and Dulvy NK (2014). Sizing up the ecological role of sharks as predators. *Mar. Ecol. Prog. Ser.* 495: 291–298.

Abstract

Forage fish (e.g. anchovies, pilchards, scads) are a major trophic link between plankton and larger predators, for which they are a major prey item. They are also intensively exploited by humans, mostly for non-food uses, and are easy to catch as they congregate in large schools from hundreds to thousands of individuals.

The effects of predator loss on lower trophic levels in pelagic ecosystems are little understood. We investigate the effects of predator abundance on the internal structure of fish schools using scads (*Decapterus* sp.) schools as a model taxon. We use baited remote underwater stereo-video systems (stereo-BRUVS) to provide the first quantitative description of pelagic fish schools in three-dimensional space, in five study locations varying in levels of predator abundance.

Our results show that contrary to expectations, schools are less tight in areas with higher predator abundance. Indeed, after controlling for fish attributes, we found that nearest neighbour distances, distance to school centre and volume increased with predator abundance, while density decreased. We hypothesise that schooling behaviour is driven by oxygen level in addition to predator abundance, and that schooling fish maintain higher distances from congeners in areas where predation risk is high to satisfy the oxygen demands associated with a flight response to potential predator attacks.